CRYSTAL GROWTH & DESIGN
2007
VOL. 7, NO. 2
300−306

From Hydrogen-Bonded Net-to-Net Framework to Twofold Interpenetrated (4,6) Net: Effect of Ligand Topology on the Supramolecular Structural Diversity

LiJun Zhou,[†,‡] YaoYu Wang,*[,†] CaiHua Zhou,[†] CuiJuan Wang,[†] QiZhen Shi,[†] and ShieMing Peng[§]

Department of Chemistry and Shaanxi Key Laboratory of Physico-inorganic Chemistry, Northwest University, Xi'an 710069, P. R. China, Department of Applied Chemistry, Xidian University, Xi'an 710071, P. R. China, and Department of Chemistry, National Taiwan University, Taipei, Taiwan

Received June 17, 2006; Revised Manuscript Received September 19, 2006

ABSTRACT: Two novel metal−organic frameworks (MOFs) of Co(II), $\{[Co(bpdc)(bpdap)]\cdot 1.5H_2O\}_n$ (**1**) and $[Co(bpdc)(Hpb)(H_2O)]_n$ (**2**) (bpdap = *N*,*N*′-bis(2-pyridyl)-2,6-diaminopyridine, H_2bpdc = biphenyl-4,4′-dicarboxylic acid, and Hpb = 2-(2-pyridyl)-benzimidazole), have been synthesized by a hydrothermal method and structurally characterized. The structure determination reveals that both **1** and **2** crystallize in a triclinic system, space group $P\bar{1}$. Complex **1** has a 1D zigzag chain where Co(II) is bridged by bpdc in alternate bis(monodentate) and bis(chelate) manners and extends to form a 2D rectangular grid (RG) framework stacking in a staggered manner through hydrogen bonding and $\pi-\pi$ interactions to form a net-to-net supramolecular network with a small channel along the *c*-axis, which accommodates the water molecules. In the case of **2**, a zigzag chain with Co(II) connected by bis(monodentate) bpdc results in a 2D RG network based on hydrogen bonding, and every two networks interlock slantwise forming a twofold interpenetrated (4,6) net framework that is stabilized by C−H···π interactions. Magnetic measurement reveals that both **1** and **2** present weakly antiferromagnetic behavior.

Introduction

Constructing solid-state entities with a predefined molecular organization constitutes the final target of crystal engineering,[1] a sub-branch of supramolecular chemistry.[2] Despite the rather severe comment,[3] crystal engineering generally and crystal engineering of metal−ligand coordination (MLC) polymers especially have been major challenging as well as rewarding areas of research due to their intriguing structural diversity and potential for many applications.[4] Rational design of the organic ligand and properly selected metal ions are the key points of constructing intriguing and useful coordination polymers.[5] On the other hand, it has been recognized that noncovalent intermolecular forces such as hydrogen bonding interactions,[6] being reasonably strong and highly directional, can be used as structure-directing tools in generating many molecular solids with novel properties.[7] Out of many approaches to gain control over the arrangement of molecules in space, incorporation of both MLC and hydrogen bonding, which can limit the possible arrangement of the molecules in the solid state with respect to one another, has been considered one of the most rational design strategies because of the structural complexity and guest entrapment induced by specific hydrogen-bonding interactions. Among the various coordination supramolecules, rectangular grid (RG) frameworks and interpenetration structures,[8,9] new types of supramolecular intertwining of infinite motifs, have gained widespread interest due to their potential applications. Our group had constructed a new type of triple-chain molecular braid architecture[10] utilizing multicarboxylate ligands, which have diverse coordination modes and are good candidates for hydrogen-bonding acceptors and donors[11] that serve as an effective building block for the formation of hydrogen-bonded molecular solids.

Scheme 1. The Sketch of Ligands bpdap and Hpb

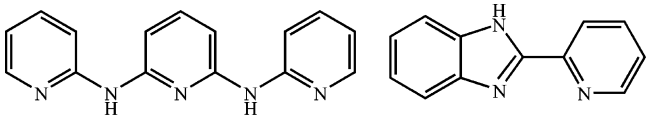

As a continuing work, with the aim to create novel supramolecular networks using both MLC and hydrogen bonding, in this paper, we react biphenyl-4,4′-dicarboxylic acid (bpdc) with cobalt(II) nitrate and two different pyridyl compounds (Scheme 1), *N*,*N*′-bis(2-pyridyl)-2,6-diaminopyridine (bpdap) and 2-(2-pyridyl)-benzimidazole (Hpb), as auxiliary ligands under hydrothermal conditions. The resultant polymers derived from these ligands are expected to self-assemble further via complementary hydrogen-bonding interactions in that the two auxiliary ligands are both eminent for producing typical hydrogen-bonding networks.[12,13] Just as expected, the obtained similar topological polymers, $\{[Co(bpdc)(bpdap)]\cdot 1.5H_2O\}_n$ (**1**) and $[Co(bpdc)(Hpb)(H_2O)]_n$ (**2**), significantly different from the coordination geometry of Co(II) and coordination modes of bridging bpdc, finally produce different extended topologies by interchain hydrogen bonding, $\pi-\pi$ stacking interactions, and C−H···π interactions. Induced by auxiliary ligands with different architectures, the 1D chain of **1** presents a hydrogen-bonded RG net-to-net staggered network when it self-organizes to form a supramolecular system, while the 1D chain of **2** displays a twofold interpenetrated (4,6) net topological structure through peculiar hydrogen-bonded interlocked interactions. This is a network transformation (Scheme 2) from a simple modulation in the chemical functionality or flexibility of the ligands, which simultaneously affects their topology and molecular properties. Furthermore, in this paper, we describe in detail the magnetic properties of the two polymers.

* To whome correspondence should be addressed. Fax: +86-29-88303798. Tel: +86-29-88373398. E-mail: wyaoyu@nwu.edu.cn.
† Northwest University.
‡ Xidian University.
§ National Taiwan University.

10.1021/cg060369l CCC: $37.00 © 2007 American Chemical Society
Published on Web 12/29/2006

Scheme 2. Network Topology of 1 and 2 in Simplified Representation

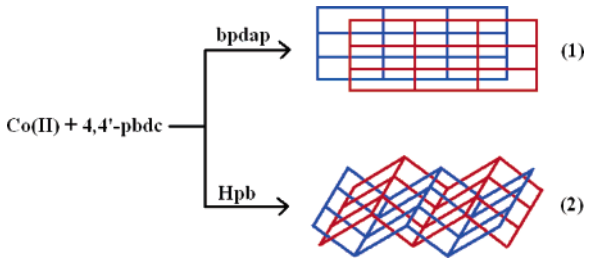

Experimental Section

General. All reagents were commercially available and were used without further purification. The bpdap was synthesized according to the reported method.[13] Elemental analyses were determined with a Perkin−Elmer 2400 CHN elemental analyzer. Infrared spectra on KBr pellets were recorded on a Nicolet 170SX FT−IR spectrophotometer in the range 4000−400 cm^{-1}. TGA analyses were recorded with a NETZSCH STA 449C microanalyzer in an atmosphere of nitrogen at a heating rate of 5 °C min^{-1}. Variable temperature magnetic susceptibility measurements were carried out on an Oxford Maglab 2000 magnetometer with an applied field of 10 kOe. Diamagnetic correction was estimated from Pascal's constants.

Synthesis of $\{[Co(bpdc)(bpdap)]\cdot 1.5H_2O\}_n$ (1). Preparation under solvothermal conditions by reaction of $Co(NO_3)_2\cdot 6H_2O$ (0.5 mmol, 145 mg), H_2bpdc (0.5 mmol, 121 mg), NaOH (1 mmol, 40.1 mg), and bpdap (0.5 mmol, 132 mg) in a mixed solution of DMF (3.0 mL), methanol (2.0 mL), and distilled water (5.0 mL) at 130 °C for 2 days produced purple block crystals in 56% yield. Anal. Calcd for $C_{29}H_{24}CoN_5O_{5.50}$: C, 59.09; H, 4.10; N, 11.88. Found: C, 59.03; H, 4.13; N, 11.80. IR (KBr cm^{-1}): 3363(m), 3060(m), 2944(w), 2856(w), 1702(m), 1573(s), 1384(s), 1294(m), 1147(m), 1083(w), 850(w), 728(w).

Synthesis of $[Co(bpdc)(Hpb)(H_2O)]_n$ (2). Synthesis was under hydrothermal conditions. A mixture of $Co(NO_3)_2\cdot 6H_2O$ (0.5 mmol, 145 mg), H_2bpdc (0.5 mmol, 122 mg), NaOH (1 mmol, 40.3 mg), Hpb (0.5 mmol, 97.9 mg), and 10.0 mL of distilled water was stirred fully in air and then sealed in a Teflon-lined stainless steel container, which was heated at 160 °C for 4 days. After the sample was cooled to room temperature, red rod-like crystals were produced in 69% yield. Anal. Calcd for $C_{26}H_{19}CoN_3O_5$: C, 60.95; H, 3.74; N, 8.20. Found: C, 60.98; H, 3.71; N, 8.24. IR (KBr cm^{-1}): 3419(s), 3067(w), 2944(m), 2856(w), 1598(s), 1536(m), 1498(w), 1427(s), 1353(w), 1296(w), 1218(m), 1128(m), 1094(w), 1016(m), 866(w), 816(w), 630(m).

X-ray Crystal Structure Determinations. X-ray diffraction data were collected on a BRUKER SMART APEXCCD diffractometer with Mo Kα monochromated radiation (λ = 0.710 73 Å) at 296(2) K. The structures were solved by direct methods and refined by full-matrix least-squares on F^2 with the SHELXL-97 program package.[14,15] The non-hydrogen atoms were located with difference Fourier synthesis, and the hydrogen atoms were generated geometrically. The crystallographic data for **1** and **2** are listed in Table 1, and selected bond lengths and angles are presented in Table 2.

Results and Discussion

Crystal Structure of $\{[Co(bpdc)(bpdap)]\cdot 1.5H_2O\}_n$ (1). The crystal structure of **1** is formed by a neutral 1D zigzag chain compose of $[Co(bpdc)(bpdap)]_n$ entities and free solvent molecules of one and a half disordered water molecules. The cobalt atoms are 4 + 2 six-coordinated in a distorted $[CoN_3O_3]$ octahedral coordination environment with three carboxyl oxygen atoms from two bpdc ligands (Co1−O1 = 2.167(4) Å, Co1−O2 = 2.253(4) Å, Co1−O3 = 2.027(4) Å) and a nitrogen atom of one bpdap (Co1−N3 = 2.084(4) Å) located in the basal sites and the other two nitrogen atoms from the bpdap (Co1−N1 = 2.092(5) Å, Co1−N5 = 2.068(4) Å) taken on the apical positions, as depicted in Figure 1a. Adjacent Co atoms are linked by bpdc ligands in alternate bis(chelate) and bis(monodentate) fashion with ABAB mode to form a 1D zigzag polymeric chain spanning along the *a*-axis. The intrachain distances of neighboring cobalt atoms bridged by bis(monodentate) or bis(chelate) bpdc are nearly identical with the value of about 15.151 and 15.133 Å, respectively. In complex **1**, the bpdap ligands extend at both sides of the chain in an antiparallel fashion, and the pyridyl rings of bpdap at each side of the chain are arranged in a parallel fashion. This orientation plays a critical role in packing into a higher network through $\pi-\pi$ stacking interactions. The three pyridyl groups of the bpdap ligand are twisted with the dihedral angle between each pair of neighboring pyridyl rings of 5.127(1)° and 12.524(2)°, smaller than that in compound $[Fe(H_2tpda)_2]Cl_2$.[16] The dihedral angle between two benzene rings of bpdc is almost 0°, indicating no torsion, which is different from many bpdc complexes,[17] and the carboxyl groups are nearly coplanar (4−5°) with their connected benzene ring. It should be mentioned that adjacent chains recognize each other to generate a 2D rectangular grid framework parallel to the *bc* plane with dimension of 18.34 × 15.13 Å (66-membered metallocyclic ring) via strong $\pi-\pi$ stacking interactions (3.342 Å) of bpdap as well as hydrogen bonding between the

Table 1. Selected Crystallographic Data for Complexes 1 and 2

	1	**2**
formula	$C_{29}H_{24}CoN_5O_{5.50}$	$C_{26}H_{19}CoN_3O_5$
formula weight	589.46	512.37
T (K)	296(2)	296(2)
crystal system	triclinic	triclinic
space group	$P\bar{1}$	$P\bar{1}$
crystal size, mm^3	0.269 × 0.125 × 0.074	0.20 × 0.18 × 0.05
a, Å	9.396(9)	8.877(3)
b, Å	10.455(10)	8.943(3)
c, Å	14.612(14)	15.517(4)
α, (deg)	70.716(12)	100.030(2)
β, (deg)	85.627(12)	90.082(2)
γ, (deg)	76.076(12)	112.987(2)
V, $Å^3$	1315(2)	1113.48(6)
Z	2	2
D_c (g/cm^3)	1.489	1.528
no. of reflns	6712	10021
θ (deg)	1.48−25.10	2.74−25.10
μ, mm^{-1}	0.705	0.816
F(000)	608	526
Limiting indices	$-11 \le h \le 10$	$-10 \le h \le 10$
	$-12 \le k \le 9$	$-10 \le k \le 10$
	$-17 \le l \le 17$	$-18 \le l \le 18$
GOF on F^2	1.054	1.067
R_1, wR_2 $[I > 2\sigma(I)]^a$	0.0636, 0.1502	0.0368, 0.0860
R_1, wR_2 (all data)^a	0.0978, 0.1749	0.0495, 0.0916

^{a} $R_1 = \sum||F_o| - |F_c||/\sum|F_o|$; $wR_2 = [\sum w(F_o^2 - F_c^2)^2/\sum w(F_o^2)^2]^{1/2}$.

Table 2. Selected Bond Lengths (Å) and Angles (deg) of 1 and 2

	Complex **1**		
Co(1)−O(3)	2.027(4)	Co(1)−N(3)	2.084(4)
Co(1)−N(1)	2.092(5)	Co(1)−O(2)	2.253(4)
Co(1)−N(5)	2.068(4)	Co(1)−O(1)	2.167(4)
N(1)−Co(1)−N(5)	174.71(17)	O(3)−Co(1)−N(5)	90.21(15)
O(3)−Co(1)−N(1)	85.70(17)	N(5)−Co(1)−O(2)	90.24(15)
N(1)−Co(1)−N(3)	92.38(17)	O(3)−Co(1)−O(2)	153.05(16)
N(1)−Co(1)−O(2)	91.89(16)	O(2)−Co(1)−O(1)	58.87(15)
N(1)−Co(1)−O(1)	87.90(16)	O(3)−Co(1)−N(3)	118.95(15)
N(5)−Co(1)−N(3)	92.53(15)	N(3)−Co(1)−O(1)	146.80(16)
N(5)−Co(1)−O(1)	89.06(15)		
	Complex **2**		
Co(1)−O(1)	1.958(2)	Co(1)−O(3)	2.069(2)
Co(1)−O(5)	1.960 (2)	Co(1)−N(1)	2.201(2)
Co(1)−N(2)	2.036(2)		
O(3)−Co(1)−N(1)	175.74(8)	O(5)−Co(1)−N(1)	91.84(8)
O(1)−Co(1)−O(3)	91.36(7)	N(2)−Co(1)−N(1)	77.21(8)
O(5)−Co(1)−O(3)	90.62(8)	O(1)−Co(1)−O(5)	124.98(10)
N(2)−Co(1)−O(3)	98.56(8)	O(1)−Co(1)−N(2)	116.40(8)
O(1)−Co(1)−N(1)	90.09(8)	O(5)−Co(1)−N(2)	117.59(10)

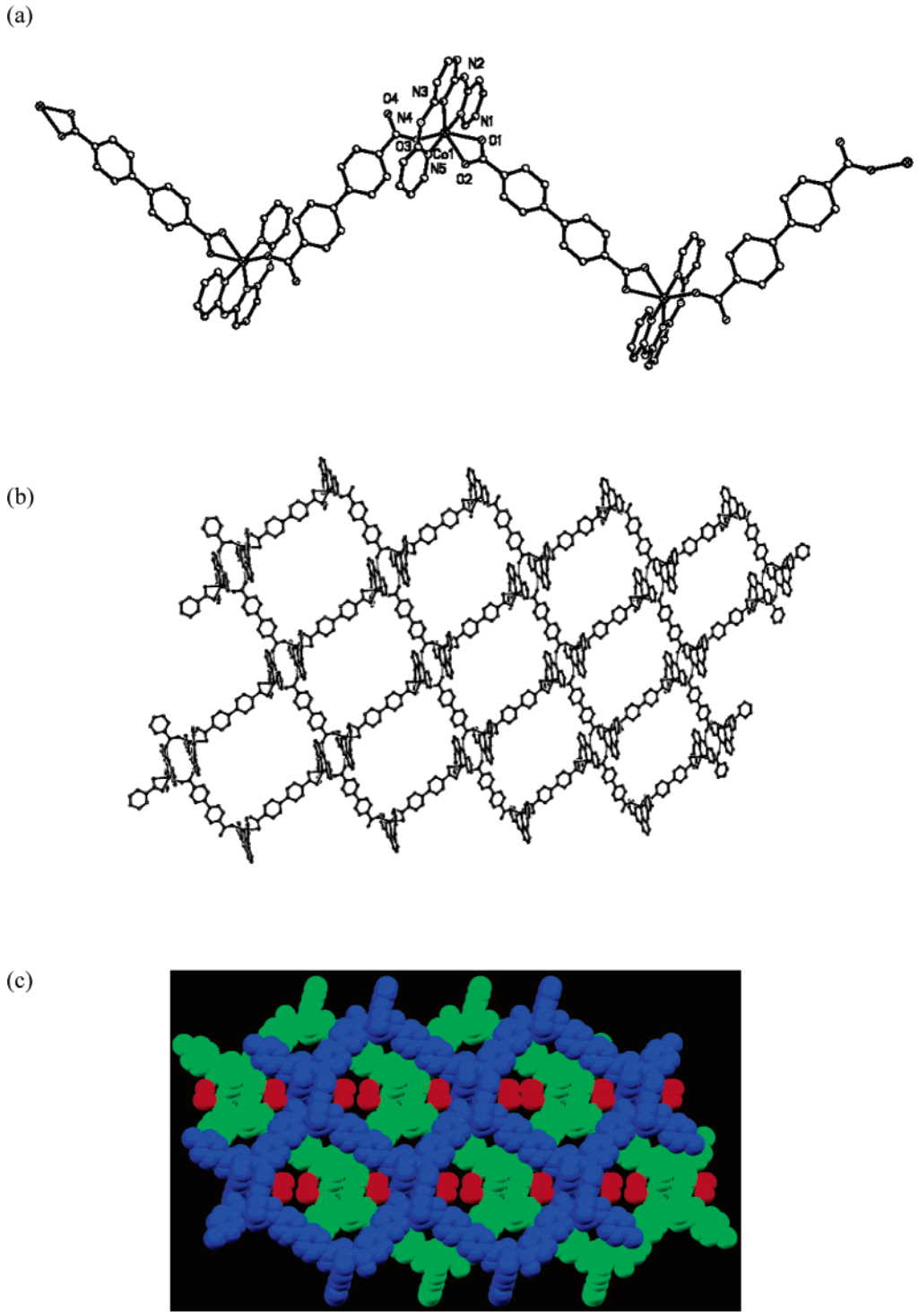

Figure 1. (a) 1D zigzag polymeric chain of complex **1** (hydrogen atoms are omitted for clarity); (b) the 2D layer in **1** with the grid size of 18.34 Å × 15.13 Å; (c) the staggered net-to-net framework linked by water dimers.

uncoordinated carboxyl oxygen of bpdc and the amido nitrogen atom from bpdap (N4···O4 = 2.845 Å, N4−H···O4 = 167.06°), as shown in Figure 1b. The grid is bigger than that of 12.0 Å × 17.4 Å constructed by the coordination bond in complex [Co(bpdc)(py)$_2$]$_n$·H$_2$O (py = pyridine).[18] The 2D grid network presents a (4,6) net in topology triggered by hydrogen-bonding interactions.

It is interesting to note that no interpenetration of the network is observed in the framework despite having such a large grid size. Instead, the available void space of the grid is occupied by free water molecules (ordered O5 and disordered O6, having strong hydrogen bonding with very short distance of 2.354 Å, which could be regarded as dimer) as well as by stacking bpdap ligands protruding from the adjacent hydrogen-bonded net. The most significant feature of **1** is that the (4,6) nets are found to pack on top of each other, displaying a slipped geometry stabilized through O_w−H···O_{coo^-} and N−H···O_w hydrogen bonds between water dimers and their connected independent sheets, as depicted in Figure 1c. To date, examples of staggered net-to-net hydrogen-bonded supromolecules are rare.[19] The slipped (4,6) nets finally condense into a 3D architecture with open channels viewed from the *b*-axis.

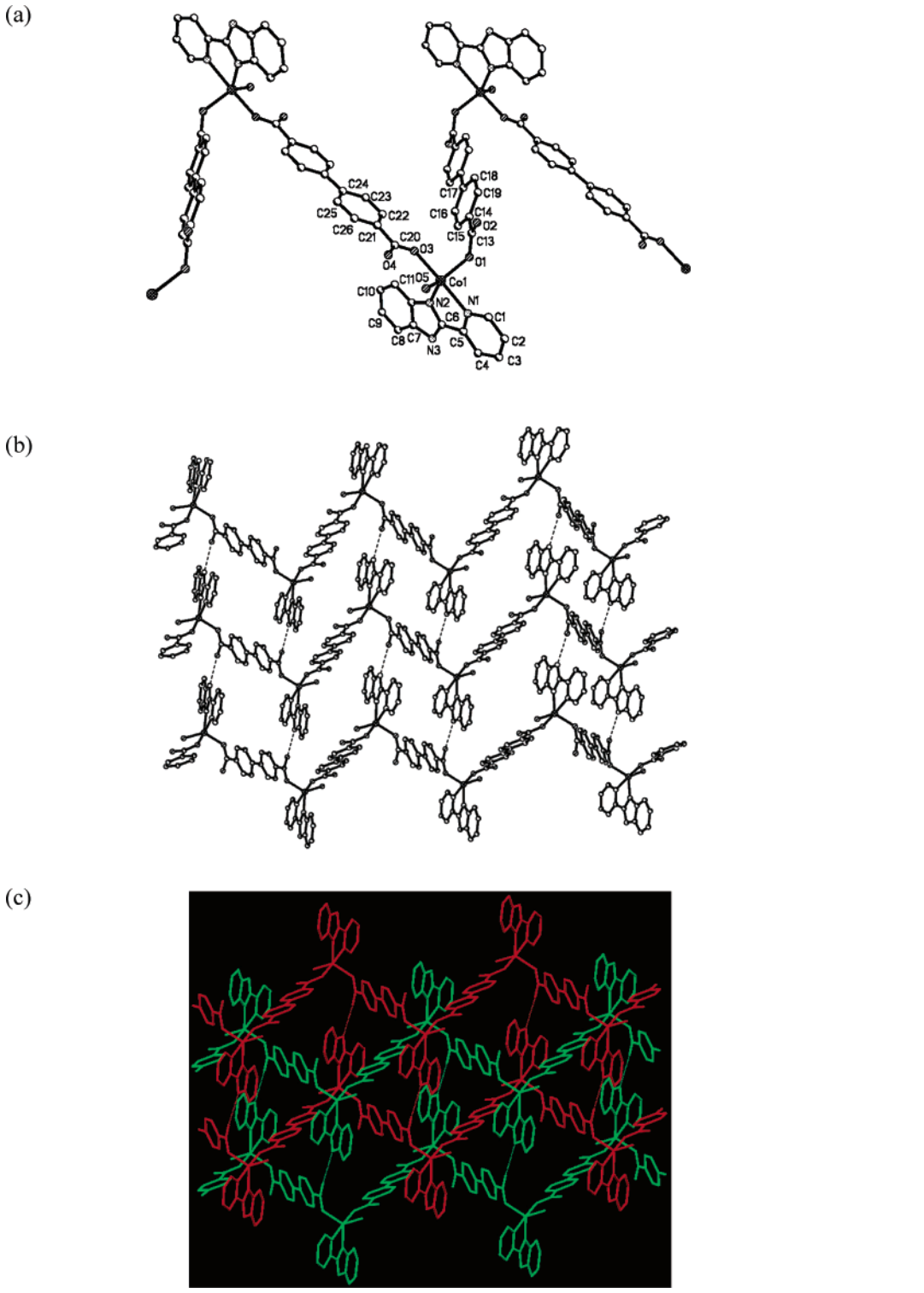

Figure 2. (a) 1D zigzag polymeric chain of complex **2** (hydrogen atoms are omitted for clarity); (b) the 2D network in **2** with the grid size of 6.7 Å × 12.3 Å and 8.9 Å × 15.6 Å; (c) the twofold interpenetrated (4,6) net in **2** formed by hydrogen bonding interlock and C−H···π interaction fastness.

Crystal Structure of $[Co(bpdc)(Hpb)(H_2O)]_n$ (2). The crystal structure of **2** is built by a 1D chain of $[Co(bpdc)(Hpb)(H_2O)]_n$ parallel to crystallographic *c*-axis, as displayed in Figure 2a. Each repeat unit consists of one cobalt atom, one Hpb ligand, one bpdc, and one coordination water molecule. Different from **1**, the cobalt atoms in **2** are 3 + 1 + 1 five-bonded to exhibit a $[CoN_2O_3]$ distorted trigonal bipyramidal environment. The equatorial plane around Co1 is built by one N atom from the Hpb ligand (Co1−N2 = 2.036(2) Å), one O atom from one carboxyl group of a bpdc ligand (Co1−O1 = 1.959(2) Å), and one O atom of one coordinated water molecule (Co1−O5 = 1.961(2) Å). The apical positions are defined by a carboxyl oxygen atom from another bpdc ligand (Co1−O3 = 2.069(2) Å) and another N atom of Hpb ligand (Co1−N1 = 2.201(2) Å). It is worth noting that there are distinct differences between crystal structures of **1** and **2**, although both of them exhibit similar topologies of 1D chain. In **2**, the environment of the cobalt atom is modified by incorporation of a bidentate Hpb

instead of tridentate bpdap in **1**, resulting in change of coordination types of bpdc from alternate bis(chelate) and bis(monodentate) modes in **1** to a uniform bis(monodentate) manner in **2**. A better insight into the chain architecture of **2** can be achieved by noting that atoms O1 and O3 from two bridging bpdc occupy the equatorial place and apical position of the connected Co centers, respectively, which results in different intrachain adjacent Co···Co distances of 14.002 and 15.645 Å, respectively (Figure 2a). Similar with **1**, Hpb ligands in **2** bristle out from the two sides of the chain and arrange in parallel at each side of the chain. The two benzene rings and their connected carboxylate groups of bpdc ligand are essential coplanar, nearly identical with those in **1**. However, the torsion angles are very dissimilar with the reported three complexes $[Cu(bpdc)(phen)(H_2O)]_n$,[20] $Cd(bpdc)(phen)_2 \cdot 2H_2O$, and $[Zn(bpdc)(H_2O)]_n$,[21,22] in which ligand bpdc also adopts a bis(monodentate) manner. In **2**, adjacent chains are intercalated in a zipper fashion generating a 2D undulating sheet containing two types of grids with sizes of ca. 6.7 Å × 12.3 Å (42-membered metallocyclic rings) and 8.9 Å × 15.6 Å (50-membered metallocyclic rings) parallel to the *ab* plane through pairs of hydrogen bonding between the uncoordinated carboxyl oxygen atoms from bpdc and the nitrogen atoms of imidazole from Hpb (N3···O2 = 2.753 Å, N3−H3A···O2 = 167.86°) (Figure 2b).

The fascinating and peculiar structural feature of **2**, however, is that the 2D undulating sheets are self-intertwined into a twofold entanglement (4,6) net when the two large void spaces within the grid are effectively filled by bpdc via the interpenetration of two independent layers. In the interpenetrating layers, every 50-membered bigger grid of one layer locks two 42-membered smaller grids from another layer; likewise every smaller grid of one layer locks two bigger grids of the adjacent layer; thus, based on the interlocked hydrogen-bonding network, a twofold interpenetrated (4,6) net is finally engendered on the *ab* plane as illustrated in Figure 2c. Besides the interlocked hydrogen bonding, the presence of two pairs of C−H···π interactions between the filling bpdc and the two benzimidazoles makes the entanglement (4,6) net tack more firmly. Compared with other entanglement structures constructed by coordination bonding,[23] complex **2** forms a rare interpenetrating architecture induced by the interlocked hydrogen-bonding network of undulating layers of self-interpenetration. The intertwining 2D layers further extend to form a 3D architecture along the *b*-axis via interchain hydrogen bonding and $\pi-\pi$ stacking interactions. Why is the extended topology of **2** clearly dissimilar from that of **1**? Comparing their structures, this may be because the undulating layers constructed by the small size of Hpb are more asymmetric and have relatively more spaces to accommodate the rod ligand bpdc shuttle in it for interpenetration than the interlayer formed by larger size of bpdap.

Thermogravimetric Analyses. Thermogravimetric analyses of complexes **1** and **2** were carried out to examine their thermal stabilities. For **1**, the first weight loss of 4.7% from 85 to 115 °C corresponds to the loss of the free water molecules in the complex (calcd 4.58%). Increasing temperature leads to the further decomposition of the bpdap molecule and bpdc anion in the compound at 275−355 °C. The final pyrolysis is completed at about 410 °C, giving a powder of cobalt oxide. For **2**, the first weight loss of 3.3% occurs at 120−225 °C, which is the loss of the coordinated water molecule (calcd 3.51%). The fact that the water molecule is released above the temperature of 120 °C in **2** suggests that the water molecule is the coordinated one instead of the crystallized one. Further decomposition begins at 265 °C and finishes at approximate 395 °C, with the remaining weight of 16.52% corresponding to the percentage of the Co and O components (calcd 15.61%).

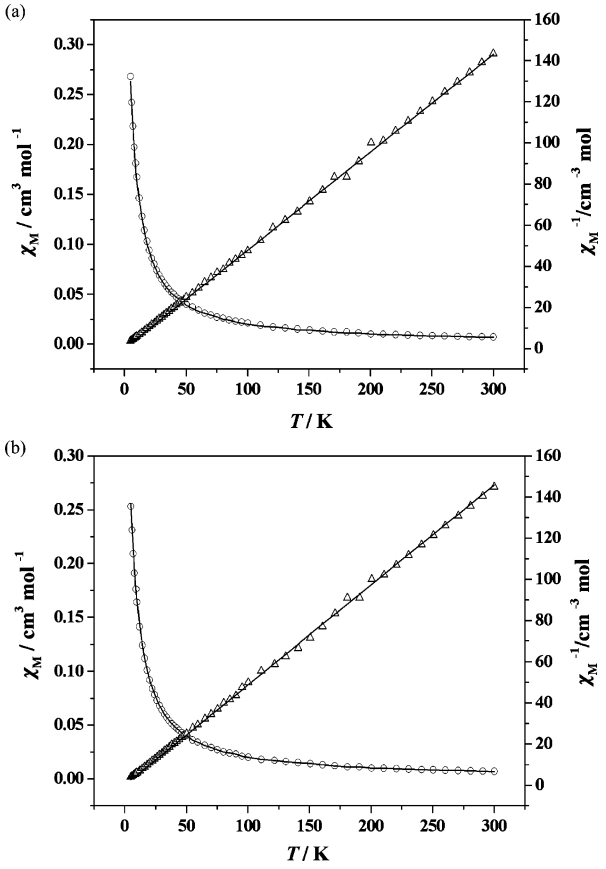

Figure 3. The magnetic plots for (a) complex **1** (experimental χ_M (○), χ_M^{-1} (△), and fitted (−)) and (b) complex **2** (experimental χ_M (○), χ_M^{-1} (△) and fitted (−)).

Magnetic Studies. Indeed, the analysis of magnetic data for cobalt complexes is complicated by the fact that single-ion effects, such as spin−orbit coupling, distortion from regular stereochemistry, electron delocalization, and crystal field mixing of excited states into the ground state, affect the magnetic properties in addition to possible a magnetic exchange interaction.[24] In spite of these difficulties, a comparative investigation of structurally analogous **1** and **2** may be helpful to learn about the contribution of different coordination modes of bridging ligands, even of different structures of auxiliary ligands. The temperature dependence of the magnetic susceptibility for compounds **1** and **2** in the range 5.0−300.0 K is shown in Figure 3 in χ_M and $1/\chi_M$ versus T form. When the temperatures are lowered, the values of χ_M for the two polymers are increased. Doubtless, the similar magnetic properties of complexes **1** and **2** indicate that there are no evident differences in the pathway of magnetic coupling interaction of the two complexes. The plots of $1/\chi_M$ versus T for complexes **1** and **2** give straight lines down to very low temperatures. Fitting the curves to the Curie−Weiss law $[1/\chi_M = (T - \theta)/C]$ gives $C = 2.10$ cm^3 K mol^{-1}, $\theta = -0.38$ K, and $r = 2.804 \times 10^{-4}$ for **1** and $C = 2.06$ cm^3 K mol^{-1}, $\theta = -0.42$ K, and $r = 2.709 \times 10^{-4}$ for **2**, where $r = \sum[(1/\chi_M)_{obs} - (1/\chi_M)_{calc}]^2/\sum[(1/\chi_M)_{obs}]^2$. The values of θ for the two complexes indicate weak antiferromagnetic interactions between the adjacent Co^{II} ($S = {}^3/_2$) ions.

Based on the structural information, the magnetic coupling mediated by van der Waals interactions between the chains could

be negligibly small. We have attempted to fit the experimental susceptibility using the classical spin Heisenberg model for a one-dimensional chain:[25]

$$\chi_M^J = \frac{N\beta^2 g^2 S(S+1)}{3kT}\frac{1+u}{1-u}$$

where $u = \coth[2JS(S+1)/(kT)] - [kT/(2JS(S+1))]$ and $S = {}^3/_2$.

The best fitting gives the parameters J, g, and R of -0.32 cm^{-1}, 2.10, and 5.69×10^{-3} for **1** and -0.34 cm^{-1}, 2.11, and 1.45×10^{-3} for **2**, where $R = \sum[(\chi_M)_{obs} - (\chi_M)_{calc}]^2/\sum[(\chi_M)_{obs}]^2$. Obviously, the results show that the antiferromagnetic interaction between the neighboring Co(II) ions in both chains is quite weak if present.

Compared with the magnitude of magnetic coupling observed in complexes of 4,4′-bipyridine, another long spacer bridge ligand, such as $[Co(acac)_2(4,4'\text{-bipy})]_n$ (acac = acetylacetone),[26] in which 4,4′-bipyridine bridges the Co(II) ions of 11.482(2) Å and $J = -0.34$, $g = 2.09$ are observed using the same fitting model,[25] the exchange constant J value of **2** is surprisingly in agreement with that. A reasonable explanation for this is that the two carboxyl groups and benzene rings of bpdc are almost coplanar in **2** instead of the twisted pyridine rings (with big dihedral angle of 34.16(17)°) in 4,4′-bipyridine complex, which contributes the conducive to magnetic orbit overlapping.

A comparison between compounds **1** and **2** indicates that the J values for **1** are a little smaller than the corresponding values of **2**. The difference may result from the fact that the metal−metal separation bridged by bpdc in **2** is shorter than that in **1**, so the magnetic exchange interaction in **2** is a little more efficient compared with that in **1**. Additionally, the difference is not so remarkable, implying little difference in mediating magnetic coupling interactions for the different coordination modes of bridge bpdc and architectures of the auxiliary ligands.

Conclusion

Two novel supramolecular architectures have been successfully designed and synthesized by the combination of coordination bonds, hydrogen bonding, $\pi-\pi$ interactions, and C−H$\cdots$ π interactions. Using different topology of auxiliary ligands leads to similar 1D zigzag topological polymers but different coordination modes of bridging ligands and coordination geometry of metal centers, ultimately generating significantly different extended RG frameworks. Complex **1** forms a 3D supramolecule with open channels extended by water dimers linking adjacent 2D layers staggered in a net-to-net framework via hydrogen-bonding self-discrimination and $\pi-\pi$ interactions. Complex **2** condenses into a twofold interpenetrated (4,6) net architecture through 2D undulating sheets self-intertwining via hydrogen-bonding interlock and C−H$\cdots\pi$ interaction fastness. A compared magnetic investigation shows almost the same antiferromagnetic behavior, demonstrating little difference for different coordination modes of bridge ligand and architectures of the auxiliary ligands in mediating magnetic coupling interactions.

Acknowledgment. This work was supported by the National Natural Science Foundation of China (Grant No. 20471048) and TRAPOYT.

Supporting Information Available: Magnetic data and crystallographic information in CIF format for complexes **1** and **2**. This material is available free of charge via the Internet at http://pubs.acs.org. X-ray crystallographic files in CIF have been deposited with the Cambridge Crystallographic Data Center, CCDC reference numbers 295165 for **1** and 295166 for **2**. Copies of this information may be obtained free of charge from The Director, CCDC, 12 Union Road, Cambridge, CB2 1EZ, UK (fax C44 1223 336033; e-mail deposit@ccdc.cam.ac.uk or http://www.ccdc.cam.ac.uk).

References

(1) Desiraju, G. R. *Crystal Engineering: The Design of Organic Solids*; Elsevier: Amsterdam, The Netherlands, 1989.
(2) (a) Lehn, J. M. *Supramolecular Chemistry, Concepts and Perspectives*; VCH: Weinheim, Germany, **1995**. (b) Lehn, J. M. *Angew. Chem., Int. Ed. Engl.* **1988**, *27*, 89.
(3) Maddox, J. *Nature (London)* **1988**, *335*, 201.
(4) (a) Yaghi, O. M.; O'Keeffe, M.; Ockwig, N. W.; Chae, H. K.; Eddaoudi, M.; Kim, J. *Nature* **2003**, *423*, 705. (b) Kitaura, R.; Seki, K.; Akiyama, G.; Kitagawa, S. *Angew. Chem., Int. Ed.* **2003**, *115*, 444. (c) Lin, W.; Evans, O. R.; Yee, G. T. *J. Solid State Chem.* **2000**, *152*, 152. (d) Evans, O. R.; Lin, W. *Chem. Mater.* **2001**, *13*, 2705. (e) Albrecht, M.; Lutz, M.; Spek, A. L.; Van, K. G. *Nature* **2000**, *406*, 970.
(5) (a) James, S. L. *Chem. Soc. Rev.* **2003**, *32*, 276. (b) Batten, S. R.; Robson, R. *Angew. Chem., Int. Ed.* **1998**, *37*, 1460.
(6) (a) Aakeröy, C. B.; Seddon, K. R. *Chem. Soc. Rev.* **1993**, *22*, 397. (b) Jeffery, G. A. *Introduction to Hydrogen Bonding*; Wiley: Chichester, U.K., 1997. (c) Jeffery, G. A.; Saenger, W. *Hydrogen Bonding in Biology and Chemistry*; Springer-Verlag: Berlin, 1993.
(7) (a) Atwood, J. L.; Barbour, L. J.; Jerga, A. *Angew. Chem., Int. Ed.* **2004**, *43*, 2948. (b) Sada, K.; Inoue, K.; Tanaka, T.; Tanaka, A.; Epergyes, A.; Nagahama, S.; Matsumoto, A.; Miyata, M. *J. Am. Chem. Soc.* **2004**, *126*, 1764. (c) Zhao, H.; Li, Y.-H.; Wang, X.-S.; Qu, Z.-R.; Wang, L.-Z.; Xiong, R.-G.; Abrahams, B. F.; Xue, Z. *Chem.—Eur. J.* **2004**, *10*, 2386. (d) McBride, M. T.; Luo, T. J. M.; Palmore, G. T. R. *Cryst. Growth Des.* **2001**, *1*, 39. (e) Holman, K. T.; Pivovar, A. M.; Swift, J. A.; Ward, M. D. *Acc. Chem. Res.* **2001**, *34*, 107.
(8) (a) Hagrman, D.; Hammond, R. P.; Haushalter, R.; Zubieta, J. *Chem. Mater.* **1998**, *10*, 2091. (b) Hou, L.; Li, D.; Shi, W.-J.; Yin, Y.-G.; Ng, S. W. *Inorg. Chem.* **2005**, *44*, 7825. (c) Maji, T. K.; Ohba, M.; Kitagawa, S. *Inorg. Chem.* **2005**, *44*, 9225.
(9) (a) Carlucci, L.; Ciani, G.; Proserpio, D. M. *Coord. Chem. Rev.* **2003**, *246*, 247. (b) Hubin, T. J.; Busch, D. H. *Coord. Chem. Rev.* **2000**, *200−202*, 5. (c) Carlucci, L.; Ciani, G.; Moret,; Proserpio, D. M.; Rizzato, S. *Angew. Chem., Int. Ed.* **2000**, *39*, 1506.
(10) Luan, X.-J.; Cai, X.-H.; Wang, Y.-Y.; Wang, C.-J.; Liu, P.; Shi, Q.-Zh.; Peng, S. M. *Chem.—Eur. J.* **2006**, *12*, 6281.
(11) (a) Zhao, B.; Yi, L.; Dai, Y.; Chen, X.-Y.; Cheng, P.; Liao, D.-Zh.; Yan, Sh.-P.; Jiang, Z.-H. *Inorg. Chem.* **2005**, *44*, 911. (b) Wörl, S.; Fritsky, I.O.; Hellwinkel, D.; Pritzkow, H.; Krämer, R. *Eur. J. Inorg. Chem.* **2005**, 759. (c) Eddaoudi, M.; Moler, D. B.; Li, H.; Chen, B.; Reineke, T. M.; O'Keeffe, M.; Yaghi, O. M. *Acc. Chem. Res.* **2001**, *34*, 319. (d) Ye, B.-H.; Tong, M.-L.; Chen, X.-M.; *Coord. Chem. Rev.* **2005**, *249*, 545.
(12) Shieh, S. J.; Chou, C. C.; Lee, G.;H.; Wang, C. C.; Peng, S. M. *Angew. Chem., Int. Ed. Engl.* **1997**, *36*, 56.
(13) (a) Xia, C.-K.; Lu, C.-Zh.; Zhang, Q.-Zh.; He, X.; Zhang, J.-J.; Wu, D.-M. *Cryst. Growth Des.* **2005**, *5*, 1569. (b) Meng, X.-G.; Song, Y.-L.; Hou, H.-W.; Fan, Y.-L.; Li, G.; Zhu, Y. *Inorg. Chem*, **2003**, *42*, 1306.
(14) Sheldrick, G. M. *SHELXL−97: Program for Structure Determination*; University of Göttingen: Göttingen, Germany, 1997.
(15) Sheldrick, G. M. *SHELXL−97: Program for Structure Refinement*; University of Göttingen: Göttingen, Germany, 1997.
(16) Yang, M. H.; Lin, T. W.; Chou, C. C.; Lee, H. C.; Chang, H. C.; Lee, G. H.; Leung, M. K.; Peng, S. M. *Chem. Commun.* **1997**, 2279.
(17) (a) Filipe A. A. P.; Yaroslav Z. K.; Andrew D. B.; João R.; Jacek K. *Eur. J. Inorg. Chem.* **2002**, 2823. (b) Zheng, S.-L.; Tong, M.-L.; Yu, X.-L.; Chen, X.-M. *J. Chem. Soc., Dalton Trans.* **2001**, 586.
(18) Pan, L.; Ching, N.; Huang, X.; Li, J. *Inorg. Chem.* **2000**, *39*, 5333.
(19) (a) Pothiraja, R.; Sathiyendiran, M.; Butcher, R. J.; Murugavel, R. *Inorg. Chem.* **2005**, *44*, 6314. (b) Zhang, G.-Q.; Yang, G.-Q.; Ma, J.-S. *Cryst. Growth Des.* **2006**, *6*, 933. (c) Takaoka, K.; Kawano, M.; Tominaga, M.; Fujita, M. *Angew. Chem., Int. Ed.* **2005**, *44*, 215. (d) Uemura, K.; Kitagawa, S.; Kondo, M.; Fukui, K.; Kitaura, R.; Chang, H.-C.; Mizutani, T. *Chem.—Eur. J.* **2002**, *8*, 3587.

(20) Zhang, S. Y.; Yu, M. X.; Zhu, L. G. *Mol. Struct*. **2004**, *699*, 101.
(21) Shi, X.; Zhu, G.-Sh; Wang, X.-H.; Li, G.-H.; Fang, Q.-R.; Wu, G.; Tian, G.; Xue, M.; Zhao, X.-J.; Wang, R.-W.; Qiu, Sh.-L. *Cryst. Growth Des*. **2005**, *5*, 207.
(22) Liang, Y.-C.; Hong, M.-Ch.; Cao, R.; Weng, J.-B.; Su, W.-P. *Inorg. Chem. Commun.* **2001**, *4*, 599.
(23) Carlucci, L.; Ciani, G.; Moret, M.; Proserpio, D. M.; Rizzato, S. *Angew. Chem., Int. Ed.* **2000**, *39*, 1506.
(24) Emori, S.; Inoue, M.; Kubo, M. *Coord. Chem. Rev.* **1976**, *21*, 1.
(25) Fisher, M. E. *Am. J. Phys*. **1964**, *32*, 343.
(26) Ma, B.-Q.; Gao, S.; Tao, Y.; Xu, G.-X. *Polyhedron* **2001**, *20*, 1255.

CG060369L